Journal of Environmental Management 366 (2024) 121930

Contents lists available at ScienceDirect

Journal of Environmental Management

journal homepage: www.elsevier.com/locate/jenvman

Research article

Intensifying the sonochemical degradation of hydrophilic organic contaminants by organic and inorganic additives

John F. Guateque-Londoño [a], Efraím A. Serna-Galvis [a,b], Judy Lee [c], Yenny P. Ávila-Torres [a,**], Ricardo A. Torres-Palma [a,*]

[a] Grupo de Investigación en Remediación Ambiental y Biocatálisis (GIRAB), Instituto de Química, Facultad de Ciencias Exactas y Naturales, Universidad de Antioquia UdeA, Calle 70 No. 52-21, Medellín, Colombia
[b] Grupo de Catalizadores y Adsorbentes (CATALAD), Instituto de Química, Facultad de Ciencias Exactas y Naturales, Universidad de Antioquia UdeA, Calle 70 # 52-21, Medellín, Colombia
[c] School of Chemistry and Chemical Process Engineering, University of Surrey, Guildford, U27XH, United Kingdom

ARTICLE INFO

Keywords:
Enhanced sonodegradation
Pollutants elimination
Ultrasonic process
Water treatment

ABSTRACT

The sonochemical system is highly effective at degrading hydrophobic substances but has limitations when it comes to eliminating hydrophilic compounds. This study examines the impact of organic and inorganic additives on improving the sonochemical degradation of hydrophilic pollutants in water. The effects of adding an organic substance (CCl_4) and two inorganic ions (Fe^{2+} and HCO_3^-) were tested. The treatment was focused on a representative hydrophilic antibiotic, cefadroxil (CDX). Initially, the sonodegradation of CDX without additives was assessed and compared with two reference pollutants more hydrophobic than CDX: dicloxacillin (DCX) and methyl orange (MO). The results highlighted the limitations of ultrasound alone in degrading CDX. Subsequently, the impact of the additives on enhancing the removal of this recalcitrant pollutant was evaluated at two frequencies (375 and 990 kHz). A significant improvement in the CDX degradation was observed with the presence of CCl_4 and Fe^{2+} at both frequencies. Increasing CCl_4 concentration led to greater CDX elimination, whereas a high Fe^{2+} concentration had detrimental effects. To identify the reactive sites on CDX towards the species generated with the additives, theoretical calculations (i.e. Fukui indices and HOMO-LUMO gaps) were performed. These analyses indicated that the β-lactam and dihydrothiazine rings on CDX are highly reactive towards oxidizing species. This research enhances our understanding of the relationship between the structural characteristics of contaminants and the sonochemical frequency in the action of additives having diverse nature.

1. Introduction

In the last decades, water consumption for different human activities has increased considerably. This leads to the generation of contamination affecting the water bodies such as lakes and rivers. Therefore, researchers have determined different inorganic (e.g., heavy metals) and organic (pharmaceuticals and personal care products (PPCPs), pesticides, and dyes) pollutants (Jacob et al., 2021; Al-Tohamy et al., 2022). PPCPs belong to the group of contaminants of emerging concern (CECs), which can be persistent or pseudo-persistent in the environment (Guoliang et al., 2022). Most of the PPCPs have environmental effects that are not completely known. For example, recent studies found that antibiotic concentrations in some rivers exceed the "safe" levels by up to 300 times (Maghsodian et al., 2022; Kuang et al., 2020), generating harmful effects on the aquatic fauna and flora. It has been reported that some pharmaceutical products can generate toxic effects in fish (Medkova et al., 2022). Also, some pharmaceutical products that can act as endocrine disruptors (Benotti et al., 2009). Similarly, these compounds can exhibit a phytotoxic activity against some plants, generating an undesired effect on the growth and development of the root (Podio et al., 2020). Due to these problems generated by CECs and their possible effect on ecosystems and even human health, the use of advanced oxidation processes (AOPs) is proposed for their elimination.

AOPs generally produce strong and non-selective hydroxyl radicals ($HO^{\bullet}$) which are highly oxidizing agents and can transform organic pollutants in water. This radical reacts with toxic organic pollutants and

* Corresponding author.
** Corresponding author.
E-mail addresses: yenny.avila@udea.edu.co (Y.P. Ávila-Torres), ricardo.torres@udea.edu.co (R.A. Torres-Palma).

https://doi.org/10.1016/j.jenvman.2024.121930
Received 4 March 2024; Received in revised form 14 June 2024; Accepted 16 July 2024
Available online 24 July 2024

transforms them into smaller non-toxic organic molecules or in some cases the contaminants are mineralized (Rayaroth et al., 2022). Other oxidizing species (e.g., reactive chlorine species (RCS)) can be generated in AOPs involving chlorine molecules or chloride ions. The RCS can promote the degradation of contaminants too (Kim et al., 2020; Cai et al., 2019). Some AOPs of great interest are photocatalysis, Fenton-based treatments, ozone-based systems, electrochemical oxidation, and sonochemical degradation. These oxidation processes are profitable technologies and give rise to active species that oxidize a variety of non-biodegradable and recalcitrant compounds, with wide application at low or high concentrations of pollutants.

Ultrasound has an advantage over other AOPs, and it is the ability to selectively degrade hydrophobic organic pollutants in complex matrices such as urine, hospital, and mineral water (Papoutsakis et al., 2015; Montoya-Rodríguez et al., 2020a,b). The ultrasound process generates hydroxyl radicals from acoustic cavitation that cleavages water molecules (Eq. (1)). The radical species can promote the degradation and enhance the biodegradability of treated water (Vassilakis et al., 2004). It is important to mention that sonochemical degradation can occur in three zones, depending on the nature of the pollutants (Sathishkumar et al., 2016). The first zone is the inner part of the cavitation bubble (where volatile substances are pyrolyzed); the second zone is the interfacial region, (therein the non-volatile hydrophobic compounds can react with the sonogenerated hydroxyl radical); and the bulk solution, in this zone the non-volatile hydrophilic molecules react to a lesser extent with the hydroxyl radical (Dalhatou et al., 2019; Liu et al., 2021; Cao et al., 2020; Jiang et al., 2002).

$$H_2O +))) \rightarrow HO^{\bullet} + H^{\bullet} \quad (1)$$

Despite the formation of strong oxidizing agents, there are drawbacks to the ultrasonic degradation of some organic molecules. For example, in the second zone, molecules with hydrophobic characteristics are closer to the cavitation bubble, where they react with the sonogenerated hydroxyl radicals promoting their fast degradation. This process is favored for frequencies from 200 to 600 kHz, due to the greater formation of hydroxyl radicals that promote the oxidation of pollutants. However, the hydrophilic compounds are localized further from the cavitation bubble, and hydroxyl radical presents minor effects on its degradation. Therefore, some extra substances could be added to the system to improve the formation of other oxidizing species in the solution, thus promoting the performance of ultrasound. For instance, the presence of iron (II) is reported to yield an extra generation of $HO^{\bullet}$ (Rahmani et al., 2019), and the addition of CCl_4 results in the formation of RCS (Dehane et al., 2021a) that can act as degrading species. Moreover, when bicarbonate and/or carbonate are added, they can lead to the production of $CO_3^{\bullet-}$ (Villaroel et al., 2014; Boutemedjet et al., 2016), which can also induce the transformation of organic pollutants.

The removal capacity of ultrasound has been studied mainly to remove hydrophobic non-volatile organic contaminants. Previous works have tested, the effect of some additives on the sonochemical degradation performance (Dehane et al., 2021a; Villaroel et al., 2014; Boutemedjet et al., 2016). Nevertheless, these works present the effects of only one additive. Moreover, the effect of additives as a function of the frequency and the effect of the chemical structure of the contaminant have not been explored yet. Besides, theoretical calculations addressed to understand the interaction of degrading species produced from the additives with the target pollutant are still scarce.

This research was focused on improving the sonodegradation of hydrophilic pollutants in the presence of different additives (Fe^{2+}, CCl_4, and HCO_3^-). The sonodegradation was tested at 375 and 990 kHz, and cefadroxil (CDX) was selected as a model of hydrophilic molecules, to evaluate the accelerating effects of the additives. Indeed, the hydrophobic response of CDX was initially verified. The CDX sonodegradation was compared with methyl orange (MO) and dicloxacillin (DCX); which were selected as reference compounds according to their hydrophobicity (Log P: 0.20, 1.93, respectively). Likewise, the effects of changes in the concentration of the additive and the target contaminant were evaluated. Then, computational analyses (Fukui indices and HOMO-LUMO gaps) were used to elucidate the sites most susceptible to the attacks on CDX by the oxidizing species formed in the sonochemical treatment. Finally, the appropriateness of the resultant solution was assessed by performing phytotoxicity and antimicrobial activity tests. We can remark that this research contributes to understanding the effects of ROS and RCS, generated from the presence of additives (Fe^{2+}, CCl_4, and HCO_3^-), under sonochemical treatment for the degradation of hydrophilic organic contaminants.

2. Materials and methods

2.1. Reagents

Sodium dicloxacillin (DCX), Cefadroxil monohydrate (CDX), and sodium methyl orange (MO) were provided by La Santé, Syntofarma S.A, and Sigma Aldrich, respectively. Acetonitrile (HPLC grade), ammonium heptamolybdate (>99.3%), methanol (HPLC grade), sodium bicarbonate (>99.0 %), potassium iodide (>99.5%), sodium hydroxide and (>99.0%) and isopropanol (HPLC grade), potassium iodide (>99.5%), ammonium heptamolybdate (>99.3%) were provided by Merck. Ferrous sulfate heptahydrate (>99.0%), formic acid (99.0%), and hydrogen peroxide (30% w/v) were provided by PanReac. CCl_4 (>99%) was provided by Sigma Aldrich. All the reagents were used as received. The solutions were prepared using distilled water. The initial pH of the solutions was adjusted to 6.1.

2.2. Reaction system

The sonochemical treatments were performed in a Meinhardt cylindrical glass reactor containing 250 mL of pollutant solution. Ultrasonic frequencies of 375 and 990 kHz at the respective power densities of 94.08 and 79.4 W L^{-1} (determined by the calorimetric method) were emitted from a transducer at the bottom of the reactor. The sonochemical reactor was connected to a Huber-Minichiller thermostatic bath and the temperature was adjusted to 20 ± 2 °C. The experimental conditions (i.e. pollutant concentrations, frequency, and power) were selected based on previous works (Serna-Galvis et al., 2019). Moreover, the range of concentrations of the additives (i.e., bicarbonate anion, Fe^{2+}, and carbon tetrachloride) were selected according to reports in other investigations (Camargo-Perea et al., 2021; Rahmani et al., 2019). All experiments were performed at least in duplicate.

2.3. Analyses

2.3.1. Chromatographic analyses

Degradation of CDX and DCX was analyzed by using a UHPLC Thermo Scientific Dionex UltiMate 3000 instrument equipped with an AcclaimTM 120 RP using an Agilent C18 column (5 μm, 4.6 mm × 150 mm) and a diode array detector. The conditions of the mobile phase are described in Table 1. On the other hand, the degradation of MO was monitored by using a Mettler Toledo UV5 spectrophotometer to 465 nm. Some physical properties of CDX, MO, and DCX are presented in Table S1, Supplementary material.

Table 1
Chromatographic conditions for the monitoring of contaminants by HPLC.

Pollutants	Mobile phase (% v/v)		Flow in isocratic mode (mL min^{-1})	Detection wavelength (nm)
	10 mM Formic acid	Acetonitrile		
DCX	50	50	0.7	225
CDX	80	20	0.5	254

2.3.2. Oxidizing species accumulation

Accumulation of sonogenerated hydrogen peroxide was estimated by iodometry (Serna-Galvis et al., 2015). An aliquot of 600 μL from the reactors was added to a quartz cell containing 1350 μL of potassium iodide (0.1 M) and 50 μL of ammonium heptamolybdate (0.01 M). After 5 min, the absorbance at 350 nm was measured using a Mettler Toledo UV5 spectrophotometer. Also, experiments were carried out to determine the formation of H_2O_2 in the presence of a CCl_4 additive. Therefore, 500 μL of sample, 500 μL of distilled water, and 50 μL of titanium (IV) oxysulfate were used, and the absorbance was determined at 412 nm after 1 min in the spectrophotometer.

Phytotoxicity against radish seeds (*Raphanus sativus*) was evaluated. For the tests, samples of 5.0 mL were taken, the samples were from the best treatments evaluated in 1T and 2T (where, T is the time when CDX is 100% degraded, and 2T means the double time required to 100% remove the pharmaceutical). The pH of the sample was adjusted to close to 6.1 with NaOH 0.1 M, thus avoiding a harmful effect on seed growth due to a very acidic medium. Then, 10 Raphanus sativus seeds were introduced in each Petri dish in the presence of the samples obtained from the processes, which were carried out in duplicate. Likewise, the radicle and hypocotyl were measured during days 1, 3, and 5 of the determination of phytoxicity. For such purpose, the ratio of seeds germinated (RSG, Eq. 2) and the ratio of root length (RRG, Eq. (3)) were determined. As a phytotoxicity parameter, the germination index (GI, Eq. (5)) was assessed according to N.J. Hoekstra et al. (2002)

$$RSG\ (\%) = \frac{Number\ of\ seeds\ germinated\ in\ sample}{Number\ of\ seeds\ germination\ in\ control} x100 \quad (3)$$

$$RRG\ (\%) = \frac{Mean\ root\ length\ in\ sample}{Mean\ root\ length\ in\ control} x100 \quad (4)$$

$$GI(\%) = \frac{RSGxRRG}{100} \quad (5)$$

Antimicrobial activity was determined by the Kirby-Bauer method, using *Staphylococcus aureus* (ATCC 6538) as the indicator bacteria. The samples to be analyzed (30 μL) were seeded on Petri dishes containing 12 mL of nutrient agar (which has been inoculated with 10 μL of *S. aureus* with an optical density of 0.600 at 580 nm). After 24 h at 37 °C in a Memmert-Schwabach incubator, the diameter of the inhibitory halo was measured with a vernier (Quimbaya-Ñañez et al., 2024).

2.4. Computational analyses

The computational calculations of Fukui indices and HOMO-LUMO gaps were done by using Gaussian 09 (quantum chemistry software). Method: ground state, DFT, B3LYP; Basis: 6–311g++ (2d, 2p). The neutral molecule was considered using the dielectric constant for water (Guateque-Londoño et al., 2020).

3. Results and discussion

3.1. Evidencing the limitations of the sonochemical system to degrade CDX

Initially, the sonochemical degradation of CDX, in distilled water, at the two ultrasound frequencies (i.e., 375 and 990 kHz) was carried out. Additionally, the control molecules (i.e., DCX, which is highly hydrophobic, and MO, which is moderately hydrophilic, according to their LogP values, Table S1) were also treated sonochemically. Fig. 1 shows the evolution of the contaminants during 30 min of treatment. It can be observed that the low frequency (375 kHz) induced a high removal percentage of contaminants (i.e. 26, 60, and 84% for CDX, MO, and DCX, respectively). Meanwhile, at the higher frequency (990 kHz), the degradation percentages were lower than at 375 kHz. At both frequencies, the degradation order was DCX > MO > CDX, indicating a correlation between the degradation order and the characteristics of the pollutant. Indeed, the results in Fig. 1 confirmed that for very hydrophilic organic pollutants there is a poor removal by ultrasound. Even the degradation is more unfavored at the highest frequency.

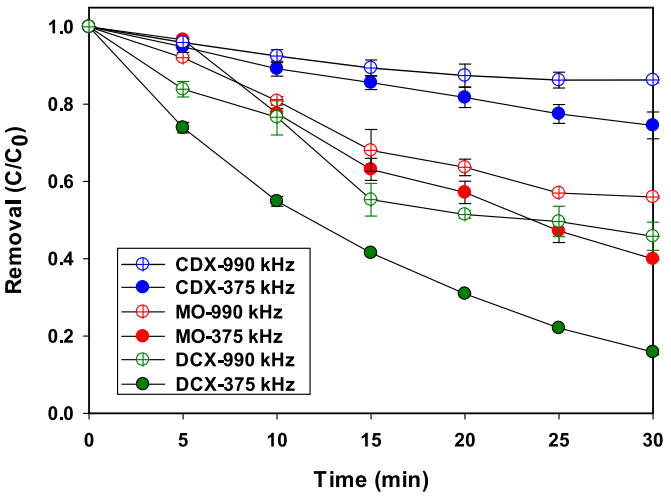

Fig. 1. Effect of structure of pollutants and frequency on the degradation by ultrasound. Experimental conditions: [Pollutant] = 30.6 μM, P = 94.08 W L^{-1} (375 kHz), P = 79.4 W L^{-1} (990 kHz), 250 mL, pH = 6.1.

The differences between the degradation at the two frequencies can be rationalized by considering that the formation of hydroxyl radicals is dependent on the ultrasonic frequency applied to the system. For frequency ranges from 200 to 500 kHz, the cavitation phenomenon favors the formation of hydroxyl radicals (Yang et al., 2008). Thereby, the degradation of the target organic pollutant is higher at 375 kHz than at 990 kHz. On the other hand, the accumulation of hydrogen peroxide, which is used as an indicator of $HO^{\bullet}$ production (Eq. (6) and Fig. S1), also supported the higher production of radicals at 375 kHz.

Besides, after 30 min of sonication of water without contaminants, the accumulation of H_2O_2 was 115 μM and 43 μM for 375 and 990 kHz, respectively. However, in the presence of CDX, it is observed that the accumulations of H_2O_2 were very close to the previously mentioned values (Fig. S1). It suggests that few hydroxyl radicals reach the hydrophilic CDX, and most $HO^{\bullet}$ is recombined before reacting with the contaminant (Eq. (6)). In contrast, in the presence of DCX, the accumulated peroxide decreased by 62% and 30%, for 375 kHz and 990 kHz, respectively; suggesting an elevate interaction between $HO^{\bullet}$ and this pollutant.

$$HO^{\bullet} + HO^{\bullet} \rightarrow H_2O_2 \quad k = 5.5x10^{9} M^{-1}\ s^{-1} \quad (6)$$

On the other hand, Table S1 indicates that the hydrophobicity of the compounds decreases as follows DCX > MO > CDX. Therefore, each contaminant is placed in different zones of the sonochemical system. Thus, based on the hydrophilic/hydrophobic nature of the contaminant, it is proposed the location of each compound regarding the cavitation bubble in the sonochemical system (Fig. S2). DCX is closer to the cavitation bubble where it reacts easily with hydroxyl radicals favoring the removal of the antibiotic (Villegas-Guzman et al., 2015).

The degradation of MO is less than DCX due to a lower value of LogP, and the hydrophobic behavior of the molecule decreases. Therefore, the MO is further away from the cavitation bubble than DCX. In turn, the CDX, which has a hydrophilic nature, is mainly placed at the solution bulk (far away from the cavitation bubble) (Camargo-Perea et al., 2021), and this supports its low removal in the sonochemical process. Additionally, the H_2O_2 generated by ultrasound cannot degrade the pollutant, as reported in previous works (Celis-Llamoca et al., 2022).

Owing to the low sonodegradation of CDX at 375 and 990 kHz, it is necessary to improve the action of the ultrasound on this hydrophilic

molecule. Thereby, we considered testing herein the strategy of CDX treatment in the presence of additives. This aspect is detailed in the next section.

3.2. Enhancement of sonodegradation of cefadroxil using additives

3.2.1. Effect of nature additives and frequency US on the degradation of hydrophilic pollutants

Firstly, to test the accelerating capability of the chosen additives (Fe^{2+}, CCl_4, or HCO_3^-), they were individually used at a concentration of 0.054 mM in the degradation process. As a criterion for the selection of the additive concentration, a previous report from our research team was employed (Serna-Galvis et al., 2016). Fig. 2 shows the effects of the additives on the degradation of CDX and the accumulation of oxidants using each additive individually at the two frequencies (375 and 990 kHz). At 375 kHz, it was not observed an accelerating or inhibiting effect on the CDX degradation in the presence of the bicarbonate anion. On the contrary, in the presence of CCl_4 or Fe^{2+}, the removal of the pollutant increased by 0.5 and 1.5 times, respectively (Fig. 2A). It was observed that the action of bicarbonate did not generate an effect on CDX degradation under sonochemical treatment at a low concentration (0.054 mM). In the case of bicarbonate anion, it could be necessary to have a high additive concentration (e.g., 2 magnitude orders, as illustrated in Fig. S3) compared to the contaminant concentration to improve the degradation (Camargo-Perea et al., 2021; Merouani et al., 2010; Pétrier et al., 2010; Serna-Galvis et al., 2022).

The accelerating effect of iron (II) is due to the Fenton reaction (Eq. (7)). The recombination of hydroxyl radicals promotes the generation of hydrogen peroxide, which accumulates at the bulk of the solution (Eq. (6)) (Pirsaheb and Moradi, 2020), and it is useful for such a reaction. From the accumulation of total oxidants in the presence and absence of the additives (inset in Fig. 2A), it was observed that the H_2O_2 concentration decreased by 87.5% in the iron presence regarding the absence of additives. This suggests that the H_2O_2 is consumed by the Fenton reaction, then generating extra hydroxyl radicals that attack CDX in the solution bulk, as represented in Fig. 3.

$$Fe^{2+} + H_2O_2 \rightarrow HO^{\bullet} + Fe^{3+} + HO^- \quad k = 2.6 - 5.8x10^8\ M^{-1}s^{-1} \tag{7}$$

In the presence of the other additive (i.e., CCl_4), an accelerating effect was also observed in the degradation of CDX. Since CCl_4 can enter inside the cavitation bubble owing to its volatile behavior (Henry's Law constant 0.034 mol kg^{-1} bar^{-1}) (Chen et al., 2012). The collapse of the cavitation bubble decomposes CCl_4 into radical species such as $Cl^{\bullet}$ (Eq. (8)). Also, CCl_4 can act as a scavenger of sonogenerated hydrogen radical (Eq. (1)) to promote the formation of species that also leads to the production of $Cl^{\bullet}$ (Eq. (9)). Then, the formation of this radical triggers a series of reactions to produce Cl_2 and HOCl (Eq. (10)–(14)), which can promote the degradation of pollutants, as depicted in Fig. 3 (Fang et al., 2014). At the same time, the sonolysis of CCl_4 leads to the accumulation of total oxidants at both frequencies (see insets of Fig. 2).

$$CCl_4 \rightarrow {}^{\bullet}CCl_3 + Cl^{\bullet} \tag{8}$$

$$CCl_4 + H^{\bullet} \rightarrow HCl + {}^{\bullet}CCl_3 \tag{9}$$

$${}^{\bullet}CCl_3 \rightarrow :CCl_2 + Cl^{\bullet} \tag{10}$$

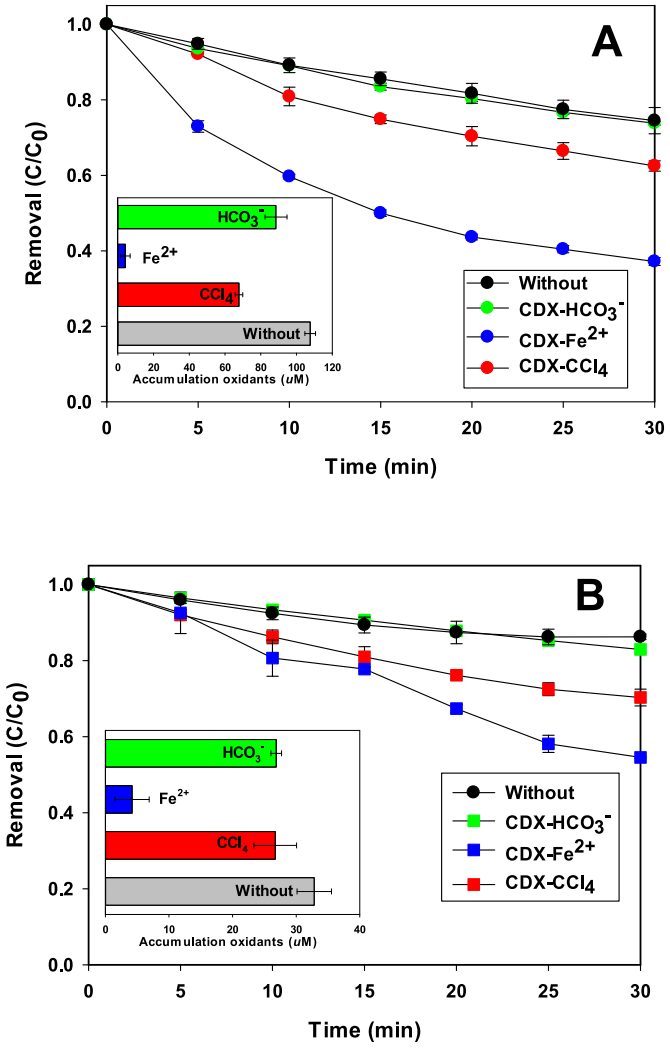

Fig. 2. Removal of CDX using ultrasound in the presence of additives. **Inset**: Accumulation of oxidants during 30 min of sonochemical treatment in the presence and absence of additives. A) at 375 kHz, B) at 990 kHz. Experimental conditions: [Pollutant] = 30.6 μM, [additive] = 0.054 mM, P = 94.08 W L^{-1} (375 kHz), P = 79.4 W L^{-1} (990 kHz), 250 mL, pH = 6.1.

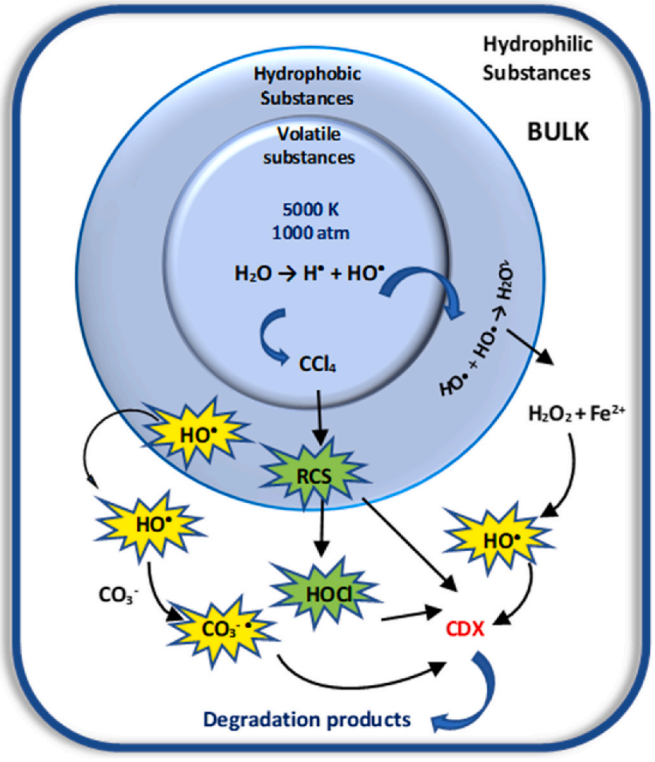

Fig. 3. Representation of the degradation routes generated by the species generated in the presence of additives.

$$^{\bullet}CCl_3 \rightarrow :CCl_2 + Cl^{\bullet} \quad (11)$$

$$^{\bullet}CCl_3 + {}^{\bullet}CCl_3 \rightarrow C_2Cl_6 \quad (12)$$

$$Cl^{\bullet} + Cl^{\bullet} \rightarrow Cl_2 \quad (13)$$

$$Cl_2 + H_2O \rightarrow HOCl + HCl \quad (14)$$

To better understand the degrading action of oxidants accumulated within the solution from the sonolysis of CCl_4, a new experiment was performed. The oxidizing capacity of this sonogenerated species was carried out. Carbon tetrachloride without the target contaminant was sonicated for 30 min, allowing it to form oxidants. Then, CDX 30.6 μM was added, and the degradation of the pollutant was analyzed (Fig. S4). A low capacity for the accumulated oxidants to remove the contaminant was evidenced, only 4.5% was removed using these conditions. At the studied pH (6.1), the presence of HOCl may predominate (Eq. (14)), and it could be responsible for the CDX degradation observed in Fig. S4. Indeed, HOCl has a redox potential ($E^{\circ} = 1.49$ V) that allows it to oxidize diverse the organic pollutants (Deborde and von Gunten, 2008).

To differentiate the RCS from ROS, the accumulation of hydrogen peroxide was determined using the specific titanium oxysulfate method (Fig. S5). It was found that the H_2O_2 accumulation is low in the presence of CCl_4 because this volatile compound enters the cavitation bubble, limiting the presence of water vapor, and thus modifying the generation of hydroxyl radicals. Additionally, HOCl can react with H_2O_2 (Eq. (15)) (Hamdaoui et al., 2022), and consequently, the accumulation of H_2O_2 is very low in the presence of CCl_4. Therefore, in the CDX sonodegradation in the presence of CCl_4, a small contribution of HOCl can be assigned. Therefore, CDX removal using sonochemistry in the presence of CCl_4 should be mainly mediated by chlorine-based radicals (e.g., $Cl^{\bullet}$) (Mi et al., 2021).

$$HOCl + H_2O_2 \rightarrow HCl + H_2O + O_2 \quad (15)$$

On the other side, the removal of CDX using 990 kHz and additives (Fig. 2B) showed a difference in degradation percentages compared to the treatment at 375 kHz. It is observed that CDX degradation increased 1.2, and 2.4 times for CCl_4 and Fe^{2+}, respectively. The accelerating effect for Fe^{2+} is correlated with the production of extra hydroxyl radicals (Eq. (7)). Despite bicarbonate anion at the tested conditions had not an accelerating effect, some hydroxyl radicals can react with HCO_3^-, decreasing a little the accumulation of H_2O_2 (Eq. (6)), as shown in the inset of Fig. 2B.

Interestingly, CCl_4 generates a major accelerating effect at 990 kHz compared with 375 kHz in the sonodegradation of CDX. In fact, at 990 kHz, the pyrolysis of CCl_4 is very high (Eq. (8)) (Dehane et al., 2021a). The formation of reactive chlorine species under the sonochemical process can be generated via two pathways: the decomposition of CCl_4 inside the bubble (Eq. (8)) and by reaction of CCl_4 with $H^{\bullet}$ (Eq. (9)). To understand the possible activation pathway of the RCS, experiments were carried out in the presence of isopropanol (ISO), as a scavenger of chlorine radicals (50 times more concentrated than CCl_4) (Wei et al., 2018). Fig. S6 shows that the degradation of CDX at 375 kHz using CCl_4 was affected by ISO, indicating that the contribution of carbon tetrachloride obeys the reaction between the hydrogen radical and CCl_4. Thus, the dominant contribution of the removal of CDX comes from the pyrolysis of the CCl_4. This is consistent with reports of the degradation of other organic contaminants under sonochemical treatment using CCl_4 (Dehane et al., 2021b; Wang et al., 2007).

3.2.2. Evaluation of the concentration of additives in the sonodegradation of CDX

After the initial evaluation of the accelerating effects at the two working frequencies, the focus of the degradation can be placed on the concentration of the additives, because it is necessary to establish the appropriate conditions that favor the removal of the elimination of the contaminant. Those additives that effectively enhanced the CDX degradation were considered. Thus, the degradation of cefadroxil was tested at different concentrations of Fe^{2+} or CCl_4. Three concentrations (0.054, 0.54, and 6.5 mM) of these additives were evaluated at the two frequencies.

The degradation enhancement index (DEI, which is calculated with the ratio between degradation percentage with additives/degradation percentage without additives (after 30 min of treatment) was determined. A DEI value less than one is considered an inhibitory effect, while DEI values greater than one have an accelerating effect on CDX degradation. Fig. 4 shows the DEI results.

It is observed a better acceleration of the CDX removal with the increase of the concentration of CCl_4 and frequency (Fig. 4). To explain the behavior of this additive as a function of concentration and frequency, it should be considered that as the CCl_4 increases the amount of the additive molecules is greater inside bubble cavitation (González-García et al., 2010). Furthermore, an increase in the concentration of CCl_4, generates an increase in the vapor pressure inside the cavitation bubble, promoting the generation of more reactive species from the pyrolysis of CCl_4 (Dehane et al., 2022). Therefore, more RCS are generated by the

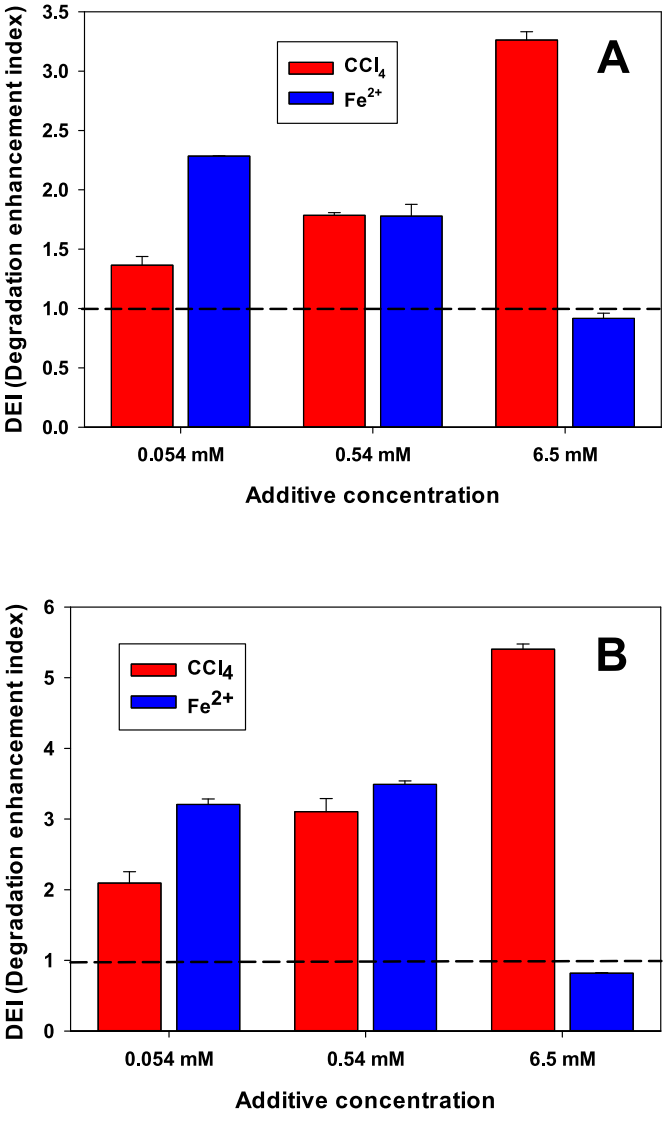

Fig. 4. Effect of additive concentration on CDX removal by sonochemical treatment (degradation enhancement index, DEI). A) Treatment a 375 kHz. B) Treatment at 990 kHz. Conditions: [Pollutant] = 30.6 μM, P = 94.08 W L^{-1} (375 kHz), P = 79.4 W L^{-1} (990 kHz), 250 mL, pH = 6.1.

CCl_4 pyrolytic route as the additive concentration is higher. Meanwhile, the number of cavitation collapses increases with the frequency (González-García et al., 2010). Therefore, CCl_4 generates more RCS by pyrolysis route at 990 kHz compared to 375 kHz. Consequently, the DEI values are higher at 990 kHz (Fig. 4B).

The addition of Fe^{2+} at different concentrations has contrary effects to the observed for CCl_4. At 375 kHz, the DEI values decreased when increasing the concentration of Fe (II) (Fig. 4A). As discussed in the previous section, the H_2O_2 generated from the recombination of hydroxyl radicals reacts with Fe (II) to give rise to the Fenton reaction. However, when the concentration of Fe (II) is increased up to 6.5 mM, inhibition effects are observed (DEI = 0.92). For this system, the pH value is 6.1. At such an experimental pH occurs the formation of iron (III) complexes that precipitate and inhibit the degradation of CDX (Pignatello et al., 2006a). Furthermore, iron (III) can act as a scavenger of the hydroxyl radical affecting the removal of CDX (Milne et al., 2013) (see also Fig. S7, which evidences that at 6.5 mM of Fe^{2+}, there was a low accumulation of oxidants).

From Fig. 4 can also be noted that the enhancing effects of iron at 990 kHz were superior to those at 375 kHz. Moreover, at 990 kHz, accelerating effects by 0.054 and 0.54 mM Fe^{2+} were found. Nevertheless, the increase of the additive up to 6.5 mM generates an opposite effect on CDX elimination (DEI: 0.92). It is important to consider that at high ultrasound frequencies (e.g., 990 kHz) the production of radicals is low, and thus a low H_2O_2 accumulation is found (Zare et al., 2023). Then, at low and moderate concentrations of Fe^{2+} (0.054 and 0.54 mM), there is the possibility of the formation of complexes between iron species and CDX, which could be more hydrophobic than the non-complexed pollutant, Fig S8.

Such complexes may be closer to the cavitation bubbles and easier to degrade, resulting in DEI values > 1 (we remark that further studies must be performed to verify this last proposal about the formation and sonochemical behavior of complexes). However, at a very high ferrous ions concentration (i.e., 6.5 mM), like at 375 kHz of frequency, the precipitation phenomena occur, leading to an inhibition of the CDX degradation (DEI: 0.81, Fig. 4B).

3.2.3. *Effect of cefadroxil concentration and pH on the action of additives*

Up to this point, the experiments were carried out at a fixed contaminant concentration of 30.6 μM. However, in actual wastewater the pollutant concentration is variable. Then, the concentration effect of CDX is investigated in this section, using the additive concentration that gave high degradation-enhancing effects (i.e., 6.5 mM CCl_4, and 0.054 mM Fe^{2+}). The frequency at 375 kHz was considered. This was selected due to at such a frequency the enhancement was lower than at 990 kHz (Fig. 4), and the modification of CDX centration could increase the DEI values.

To understand the effect of the concentration of the contaminant and the initial pH of the solution, experiments were carried out under the sonochemical treatment in the presence of the additives, Fig. S9. Fig. 5A compares the DEI of CDX at two concentrations (0.31 and 30.6 μM) of each additive. The DEI values at both CDX concentrations were close when using CCl_4. However, the pseudo-first-order constant indicates that at 30.6 μM the process is faster than at 0.31 μM (0.979 min^{-1} and 0.2375 min^{-1}, respectively). At the lowest CDX concentration, there are possible reactions of some chlorine species with hydrogen peroxide in the bulk of the solution (Eqs. (16) and (17)) (Li et al., 2022; X. Lu et al., 2022a), thus interfering with the CDX degradation kinetics.

In the meantime, Fig. 5B illustrates the comparison of the impact of pH under acidic and basic conditions (pH 3.1 and 9.1, respectively), about the pH evaluated in earlier sections. The DEI for CCl_4 remained consistent across the various pH levels examined, suggesting a minimal influence on the additive's efficacy during sonochemical treatment. Conversely, Fe^{2+} exhibited greater CDX degradation at lower pH levels, whereas its effectiveness decreased in more alkaline environments.

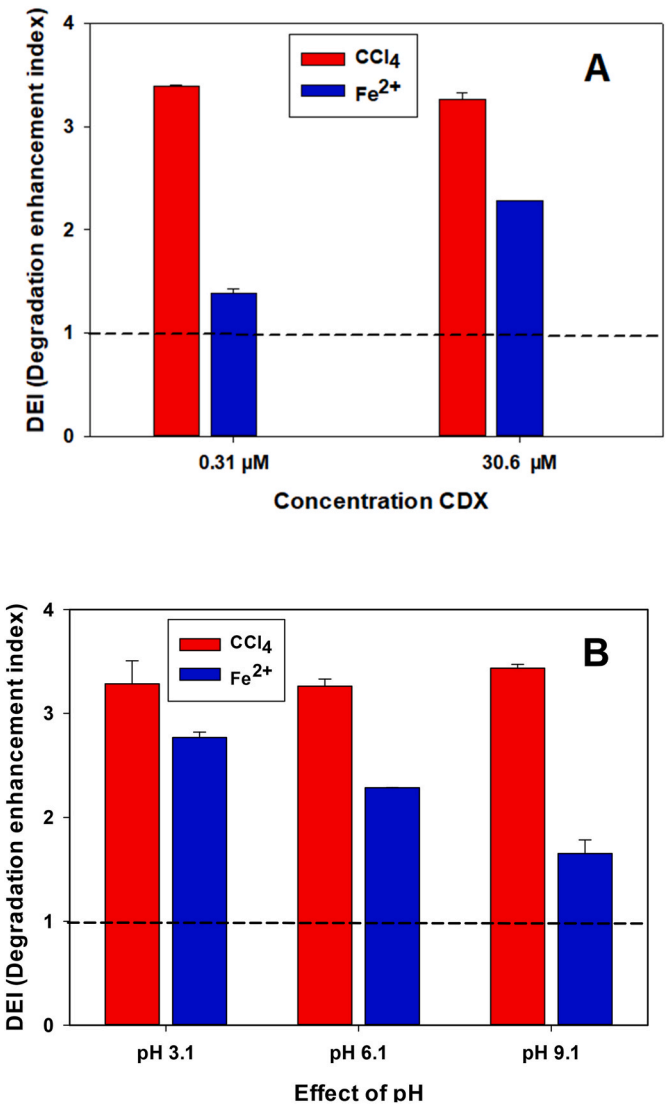

Fig. 5. Effect of concentration CDX and pH in the action of additives in sonochemical treatment. A) CDX concentration, B) Effect of pH at [CDX] = 30.6 μM. Conditions: $[CCl_4]$ = 6.5 mM, $[Fe^{2+}]$ = 0.054 mM, P = 94.08 W L^{-1}, V = 250 mL, and pH = 6.1.

$$Cl_2 + H_2O_2 \rightarrow 2H^+ + O_2 + 2Cl^- \quad (16)$$

$$ClO^- + H_2O_2 \rightarrow O_2 + H_2O + 2Cl^- \quad (17)$$

A decrease in the degradation enhancement index in the presence of iron (II) is observed at 0.31 mM regarding 30.6 mM of CDX (Fig. 5A). This is due to at the low concentration of CDX, this compound is located far from the cavitation bubble. Therefore, at the lower CDX concentration the reaction of the hydroxyl radical with CDX is lesser since a scavenger effect of hydroxyl radicals can also occur with iron (II). On the other hand, the modification of the pH at more acidic or basic values generates a change in the LogP of the cefadroxil molecule (i.e. −0.20 in acidic medium and −3.15 in basic medium) allowing it to be closer or further from the cavitation bubble, respectively (Montoya-Rodríguez et al., 2020a,b). For the sono-Fenton system, it is observed that at acidic pH a greater DEI is obtained, due to 2 main factors. First, pH 3.1 is closer to the optimal conditions to promote the Fenton reaction, since it allows the stabilization of Fe^{2+} in solution. Secondly, at the lower pH the CDX molecule is more hydrophobic compared to pH 6.1, therefore, CDX is closer to the cavitation bubble, which promotes a greater reaction with

the hydroxyl radicals generated. However, at pH 9.1 the degradation decreased due to the formation of insoluble iron species that are not very active in the Fenton reaction, in such a way that they inhibit the reaction to generate $HO^{\bullet}$ (Pignatello et al., 2006b). In the case of CCl_4, interestingly, pH does not exert significant effects on the removal of CDX, because the RCS are generated inside the cavitation bubble without effects of the pH of the solution. Moreover, the pH of the solution was monitored over time for each evaluated system (Fig. S9), showing that in the presence of Fe^{2+} the solution ends with an acidic pH due to the nature of the ultrasound that generates the formation of species such as HNO_2 or HNO_3 from the N_2 dissolved in the water (Supeno and Kruus, 2000). While in the presence of CCl_4 the pH tends to be acidic due to the aforementioned and to the further formation of species such as HOCl or HCl (accumulation of chloride in reaction time Fig. S10) (Djaballah et al., 2023). Finally, given that the process in the presence of CCl_4 generates the formation of chloride (Fig. S10) and the counterion of Fe^{2+} is SO_4^{2-}, the effect of these ions on the CDX elimination was evaluated (Fig. S11). It was evident that at the tested concentrations, they did not play an important role in the degradation of CDX, since they are not able to generate oxidizing species capable to degrade the contaminant.

3.3. Analysis of CDX susceptibility to attacks by radical species

To elucidate susceptible sites to attacks of radicals, the Fukui indices of CDX were determined via density functional theory (DFT) (Lai et al., 2023) (Table 2). A high f^+ value indicates which atom is more prone to nucleophilic reactive species (Bryantsev et al., 2011), a large f^- indicates the atom that is more susceptible to electrophilic reactive species, and a high f^0 indicates that the atomic site tends to react with radicals.

In addition to the Fukui indices, the HOMO energy, LUMO energy, and HOMO-LUMO energy difference (GAP, which indicates if a molecule is polarizable and reactive) for CDX were also calculated (Fig. 6A). A low GAP (0.6926 eV), as observed for CDX. Then, to predict the attacks of the main species (i.e., $HO^{\bullet}$, $Cl^{\bullet}$, $Cl_2^{\bullet-}$, $ClO^{\bullet}$, HOCl) involved in the CDX degradation in the presence of Fe^{2+} and CCl_4 additives, the molecular sites most susceptible to attacks by such species were determined by calculations of the GAP values (Fig. 6B).

The Fukui indexes revealed that atoms 9N (on primary amine), 4O, 5O, 18C (on carboxylic acid), 1S, 13C, 115 C (on dihydrothiazine ring), 12C (belonging to the β-lactam ring), 3O,16C (on amide), 6O (on phenol), 21C, 23C, 24C, 25C (aromatic ring) of cefadroxil have the highest values for f°. This suggests that such regions on CDX are the most susceptible to transformations by different radicals sonogenerated. These results agree with other investigations, in which the degradation products for β-lactam antibiotics are generated by attacking different radicals to the atomic sites indicated by the high f° values (Aydogdu and Hatipoglu, 2023). For example, decarboxylation in the carboxylic acid; oxidation of the amino group, hydroxylation on the aromatic ring, attack

Table 2
Results of computational analysis (Fukui function indices) for Cefadroxil*.

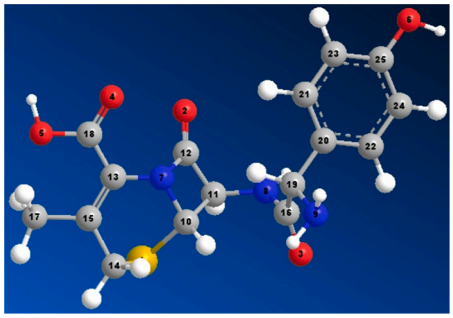

Atoms	No	f^+	f^-	f°
S	1	0.068	0.088	0.078
O	2	0.072	0.017	0.044
O	3	0.014	0.041	0.027
O	4	0.100	0.003	0.051
O	5	0.193	0.007	0.100
O	6	0.001	0.051	0.026
N	7	-0.010	0.003	-0.003
N	8	-0.008	0.004	-0.002
N	9	0.001	0.215	0.108
C	10	-0.001	-0.004	-0.003
C	11	0.007	0.001	0.004
C	12	0.057	0.008	0.033
C	13	0.047	0.007	0.027
C	14	-0.011	-0.003	-0.007
C	15	0.073	0.005	0.039
C	16	0.007	0.013	0.010
C	17	-0.009	0.000	-0.005
C	18	0.105	0.001	0.053
C	19	0.000	-0.041	-0.020
C	20	0.000	0.019	0.009
C	21	0.001	0.018	0.010
C	22	0.002	0.011	0.006
C	23	0.001	0.031	0.016
C	24	0.002	0.028	0.015
C	25	0.001	0.018	0.010

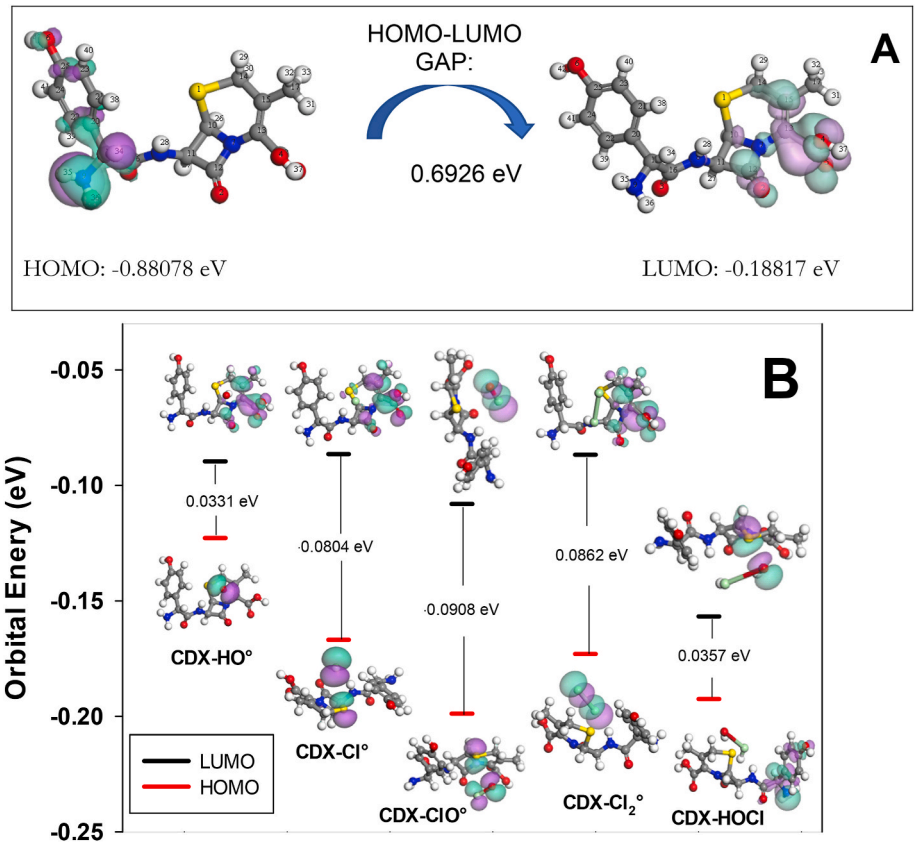

Fig. 6. Determination of the GAPs for cefadroxil. A) HOMO-LUMO energy difference for CDX alone. B) GAP generated in the presence of oxidizing species. Note: Atoms blue, yellow, and red correspond to nitrogen, sulfur, and oxygen, respectively.

on the β-lactam ring, and dihydrothiazine ring have been reported (He et al., 2014).

Fig. 6A shows that the HOMO of CDX is mainly located on the primary amine, while the LUMO of CDX is located on the β-lactam ring and dihydrothiazine ring (Diki et al., 2018). These results suggest that those rings are more susceptible to attacks by the generated oxidant species. Likewise, the GAP for the cefadroxil molecule was determined, obtaining a value of 0.6926 eV. Thus, compounds with relatively smaller GAP energies may be more likely attacked by oxidizing species (Won et al., 2015; Uzzaman et al., 2019).

On the other hand, the HOMO and LUMO energies, for the attack of the main degrading species ($HO^{\bullet}$, $Cl^{\bullet}$, $ClO^{\bullet}$, $Cl_2^{\bullet-}$, and HOCl) to the cefadroxil molecule, were calculated (Fig. 6B). Fig. 6B also shows the molecular sites of CDX more probable to be attacked by the different species that promote the degradation. The GAP value generated between CDX and $HO^{\bullet}$ is 0.031 eV (the lowest), indicating that the pollutant molecule is susceptible to act as an acceptor against this radical species where degradation occurs mainly on the dihydrothiazine ring. This also agrees with the Fukui indices for radical attacks (f°) that have the highest values in the dihydrothiazine moiety. Additionally, due to the high redox potential of the radical ($E^{\circ} = 2.8$ V), the attack can occur on both HOMO and LUMO regions.

On the other hand, the chlorine radical species are less oxidizing (2.4 V–$Cl^{\bullet}$, 2.0 V–$ClO^{\bullet}$, 1.5–1.8 V–$Cl_2^{\bullet-}$) but more selective than the hydroxyl radical. This is evidenced by a larger gap. According to theoretical calculations, $HO^{\bullet}$ and $Cl^{\bullet}$ initial reactions occur via addition to unsaturated bonds or H-abstraction (from hydrogen bonded to N or O) with target compounds in an aquatic environment (Guo et al., 2017). These reactive species preferentially react with compounds containing electron-rich moieties. Besides, HOCl presents a smaller GAP in comparison with the chlorine radical species. In this last case, the HOMO is located in the amine group of CDX, which is also supported by the affinity of the hypochlorous acid for the compounds with nitrogen such as amines and amides (Moreno-Palacios et al., 2019).

3.4. *Treatment extent: antimicrobial activity and phytotoxicity evolutions of treated solutions*

To evaluate the appropriateness of the resultant water after treatment, antimicrobial activity, and phytotoxicity tests were performed. Thereby, *S. aureus* (gram-positive bacteria) and *Raphanus sativus* (a model seed) were used to determine the effect of the resultant solution of CDX after the treatment by the ultrasound system (at 375 kHz) in the presence of CCl_4 or Fe^{2+}. The concentrations of additives were selected according to the conditions that led to the highest degradation of the antibiotic (6.5 mM CCl_4 and 0.054 mM Fe^{2+}, Section 3.3). Thus, the germination index (GI, Fig. 7) and removal of the antimicrobial activity (AA, Fig. S12) were used as parameters to determine the toxic effects of the resultant solutions after the treatment.

The evolution of the antimicrobial activity indicated that the degradation products generated by the Fe^{2+} and CCl_4 additives at 2T eliminated the antibiotic activity against *S. Aureus* (Fig. S11). This can be associated with the nature of the oxidants generated (ROS and RCS), which are able to attack the β-lactam and dihydrothiazine rings of CDX (as described in the previous section). I.e., the regions on CDX responsible for the antimicrobial activity, thus leading to the AA elimination. It can be highlighted that our result is similar to those reported in other investigations in which attacks on the β-lactam ring of other antibiotics induce the loss of biological activities of the antibiotic molecule (Z. Lu et al., 2022b; Ribeiro et al., 2018).

On the other hand, Fig. 7 shows the evolution of GI at different sonochemical treatment times (1T: the time required to achieve 100% of CDX degradation, and 2T: 2-fold T) in the presence of the additives. The results indicate that at 1T of treatment, the ultrasound/additive system

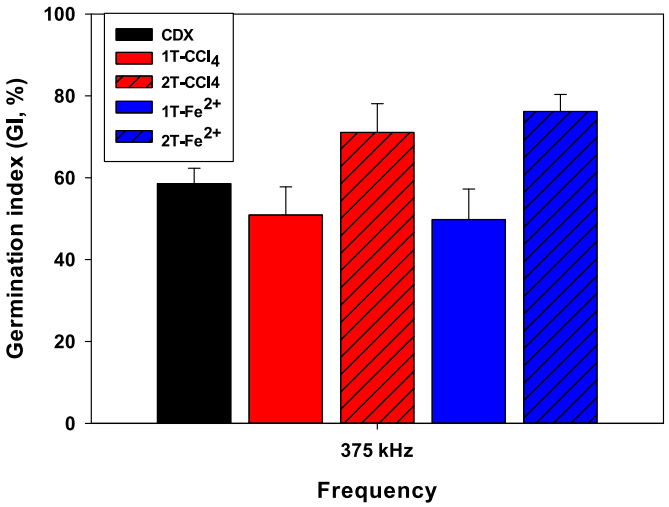

Fig. 7. The extent of sonochemical treatment with additives in distilled water. Evolution of the toxicity (GI, germination index) of cefadroxil and by-products of degradation against radish seeds. Note: the time was normalized concerning the time necessary to completely degrade cefadroxil. Then, T is the time when CDX is 100% degraded, and 2T means the double time required to 100% remove the pharmaceutical. Experimental conditions as described in Fig. 4.

did not remove the phytotoxic activity toward the indicator seed. However, when the treatment time is extended to 2T, there is an increase in the GI for both additives compared to CDX without treatment. Then, it can be proposed that the by-products generated at long treatment periods of sonication in the presence of CCl_4 or Fe^{2+} are less phytotoxic than the parent compound (Kishimoto, 2019). Therefore, these results of AA and GI suggest that the treated water could be employed in crop irrigation systems.

4. Conclusions

The use of additives offers an opportunity to improve the limitations of the ultrasound process for the degradation of hydrophilic contaminants. In the present research, the results showed that each additive has a different pathway to enhance the degradation of CDX (a model of hydrophilic compounds). CCl_4 and Fe^{2+} exhibited enhancing effects but HCO_3^- did not induce significant improvement of the sonodegradation. The frequency played a relevant role in the effect of the additives. Indeed, CCl_4 presented a synergistic effect by increasing the CDX degradation at both studied frequencies at different levels, leading to the formation of reactive chlorine species available for the degradation of the target antibiotic. The rise of CCl_4 increased the CDX elimination. On the contrary, Fe^{2+} exhibited an inhibitory effect by increasing the concentration of this additive due to a radical scavenging action. On the other hand, the computational analyses allowed us to propose the attacks of the different oxidant species generated in the presence of additives on the β-lactam and dihydrothiazine moieties of CDX. Finally, the toxicity tests showed that for long treatment times, the activity of the treated solutions against *S. aureus* and *R. sativus* is removed, and the resultant water could be used for crop irrigation. Therefore, the results contribute to the understanding of the effect of the chemical structure of some contaminants of emerging concern under sonochemical treatment, in addition to the opportunity to use substances that are present in water that promote the degradation of recalcitrant contaminants.

CRediT authorship contribution statement

John F. Guateque-Londoño: Writing – original draft, Methodology, Investigation, Data curation. **Efraím A. Serna-Galvis:** Writing – review & editing, Supervision, Methodology, Formal analysis, Conceptualization. **Judy Lee:** Writing – review & editing, Project administration, Funding acquisition, Conceptualization. **Yenny P. Ávila-Torres:** Writing – review & editing, Supervision, Software, Methodology, Conceptualization. **Ricardo A. Torres-Palma:** Writing – review & editing, Resources, Funding acquisition, Conceptualization.

Declaration of competing interest

The authors declare that they have no known competing financial interests or personal relationships that could have appeared to influence the work reported in this paper.

Data availability

Data will be made available on request.

Acknowledgements

This research was funded by MINCIENCIAS COLOMBIA, grant No. 1115-852-69594 (PRO-CEC-AGUA); and the ROYAL SOCIETY-UK, project "Sound" methods of remediating emerging contaminants in hospital wastewater (ICA/R1/191053).

Appendix A. Supplementary data

Supplementary data to this article can be found online at https://doi.org/10.1016/j.jenvman.2024.121930.

References

Al-Tohamy, R., Ali, S.S., Li, F., Okasha, K.M., Mahmoud, Y.A.G., Elsamahy, T., Jiao, H., Fu, Y., Sun, J., 2022. A critical review on the treatment of dye-containing wastewater: ecotoxicological and health concerns of textile dyes and possible remediation approaches for environmental safety. Ecotoxicol. Environ. Saf. 231, 113160 https://doi.org/10.1016/j.ecoenv.2021.113160.

Aydogdu, S., Hatipoglu, A., 2023. Aqueous degradation of 6-APA by hydroxyl radical: a theoretical study. J. Mol. Model. 29 (8), 1–12. https://doi.org/10.1007/s00894-023-05636-y.

Benotti, M.J., Trenholm, R.A., Vanderford, B.J., Holady, J.C., Stanford, B.D., Snyder, S. A., 2009. Pharmaceuticals and endocrine disrupting compounds in U.S. drinking water. Environ. Sci. Technol. 43 (3), 597–603. https://doi.org/10.1021/es801845a.

Boutemedjet, S., Hamdaoui, O., Merouani, S., Pétrier, C., 2016. Sonochemical degradation of endocrine disruptor propylparaben in pure water, natural water, and seawater. Desalination Water Treat. 57 (57), 27816–27826. https://doi.org/10.1080/19443994.2016.1177600.

Bryantsev, V.S., Giordani, V., Walker, W., Blanco, M., Zecevic, S., Sasaki, K., Uddin, J., Addison, D., Chase, G.V., 2011. Predicting solvent stability in aprotic electrolyte Li-air batteries: nucleophilic substitution by the superoxide anion radical (O2 •). The Journal of Physical Chemistry A Scheme 115, 12399–12409.

Cai, W.W., Peng, T., Zhang, J.N., Hu, L.X., Yang, B., Yang, Y.Y., Chen, J., Ying, G.G., 2019. Degradation of climbazole by UV/chlorine process: kinetics, transformation pathway and toxicity evaluation. Chemosphere 219, 243–249. https://doi.org/10.1016/j.chemosphere.2018.12.023.

Camargo-Perea, A.L., Serna-Galvis, E.A., Lee, J., Torres-Palma, R.A., 2021. Understanding the effects of mineral water matrix on degradation of several pharmaceuticals by ultrasound: influence of chemical structure and concentration of the pollutants. Ultrason. Sonochem. 73 https://doi.org/10.1016/j.ultsonch.2021.105500.

Cao, H., Zhang, W., Wang, C., Liang, Y., 2020. Sonochemical degradation of poly- and perfluoroalkyl substances – a review. Ultrason. Sonochem. 69 (June), 105245 https://doi.org/10.1016/j.ultsonch.2020.105245.

Celis-Llamoca, K., Serna-Galvis, E.A., Torres-Palma, R.A., Nieto-Juárez, J.I., 2022. High-frequency ultrasound processes as alternative methods for degrading meropenem antibiotic in water. MethodsX 9 (August), 101835. https://doi.org/10.1016/j.mex.2022.101835.

Chen, F., Freedman, D.L., Falta, R.W., Murdoch, L.C., 2012. Henry's law constants of chlorinated solvents at elevated temperatures. Chemosphere 86 (2), 156–165. https://doi.org/10.1016/j.chemosphere.2011.10.004.

Dalhatou, S., Laminsi, S., Pétrier, C., Baup, S., 2019. Competition in sonochemical degradation of Naphthol Blue Black: presence of an organic (nonylphenol) and a mineral (bicarbonate ions) matrix. J. Environ. Chem. Eng. 7 (1), 102819 https://doi.org/10.1016/j.jece.2018.102819.

Deborde, M., von Gunten, U., 2008. Reactions of chlorine with inorganic and organic compounds during water treatment-Kinetics and mechanisms: a critical review. Water Res. 42 (1–2), 13–51. https://doi.org/10.1016/j.watres.2007.07.025.

Dehane, A., Merouani, S., Hamdaoui, O., 2021a. Carbon tetrachloride (CCl4) sonochemistry: a comprehensive mechanistic and kinetics analysis elucidating how

CCl4 pyrolysis improves the sonolytic degradation of nonvolatile organic contaminants. Separ. Purif. Technol. 275 (March), 118614 https://doi.org/10.1016/j.seppur.2021.118614.
Dehane, A., Merouani, S., Hamdaoui, O., 2021b. Effect of carbon tetrachloride (CCl4) sonochemistry on the size of active bubbles for the production of reactive oxygen and chlorine species in acoustic cavitation field. Chem. Eng. J. 426, 130251 https://doi.org/10.1016/j.cej.2021.130251.
Dehane, A., Merouani, S., Hamdaoui, O., 2022. The effect of liquid temperature on bubble-size distribution in the presence of power ultrasound and carbon tetrachloride. Appl. Water Sci. 12 (12) https://doi.org/10.1007/s13201-022-01781-6.
Diki, N., Silvère, Y., Valery, B.K., Guy-richard, M., Augustin, O., 2018. Cefadroxil drug as corrosion inhibitor for aluminum in 1 M HCl medium : experimental and theoretical studies. J. Appl. Chem. 11 (4), 24–36. https://doi.org/10.9790/5736-1104012436.
Djaballah, M.L., Belghit, A., Dehane, A., Merouani, S., Hamdaoui, O., Ashokkumar, M., 2023. Radicals ([rad]OH, Cl[rad], ClO[rad] and Cl2[rad]−) concentration profiles in the intensified degradation of reactive green 12 by UV/chlorine process: chemical kinetic analysis using a validated model. J. Photochem. Photobiol. Chem. 439 (January), 114557 https://doi.org/10.1016/j.jphotochem.2023.114557.
Fang, J., Fu, Y., Shang, C., 2014. The roles of reactive species in micropollutant degradation in the UV/free chlorine system. Environ. Sci. Technol. 48 (3), 1859–1868. https://doi.org/10.1021/es4036094.
González-García, J., Sáez, V., Tudela, I., Díez-Garcia, M.I., Esclapez, M.D., Louisnard, O., 2010. Sonochemical treatment of water polluted by chlorinated organocompounds. Water (Switzerland) 2 (1), 28–74. https://doi.org/10.3390/w2010028. A review.
Guateque-Londoño, J.F., Serna-Galvis, E.A., Ávila-Torres, Y., Torres-Palma, R.A., 2020. Degradation of losartan in fresh urine by sonochemical and photochemical advanced oxidation processes. Water (Switzerland) 12 (12). https://doi.org/10.3390/w12123398.
Guo, K., Wu, Z., Shang, C., Yao, B., Hou, S., Yang, X., Song, W., Fang, J., 2017. Radical chemistry and structural relationships of PPCP degradation by UV/chlorine treatment in simulated drinking water. Environ. Sci. Technol. 51 (18), 10431–10439. https://doi.org/10.1021/acs.est.7b02059.
Guoliang, Y., Fang, D., Chowdhury, A., Aixin, Z., Sajid, M., 2022. Persistent organic pollutants in Chinese waterways: occurrence, remediation, and epidemiological perspectives: POPs in Chinese waterways. Regional Studies in Marine Science 56, 102688. https://doi.org/10.1016/j.rsma.2022.102688.
Hamdaoui, O., Merouani, S., Ait Idir, M., Benmahmoud, H.C., Dehane, A., Alghyamah, A., 2022. Ultrasound/chlorine sono-hybrid-advanced oxidation process: impact of dissolved organic matter and mineral constituents. Ultrason. Sonochem. 83, 105918 https://doi.org/10.1016/j.ultsonch.2022.105918.
He, X., Mezyk, S.P., Michael, I., Fatta-Kassinos, D., Dionysiou, D.D., 2014. Degradation kinetics and mechanism of β-lactam antibiotics by the activation of H2O2 and Na2S2O8 under UV-254nm irradiation. J. Hazard Mater. 279, 375–383. https://doi.org/10.1016/j.jhazmat.2014.07.008.
Hoekstra, N.J., Bosker, T., Lantinga, E.A., 2002. Effects of cattle dung from farms with different feeding strategies on germination and initial root growth of cress (Lepidium sativum L.). Agric. Ecosyst. Environ. 93 (1–3), 189–196. https://doi.org/10.1016/S0167-8809(01)00348-6.
Jacob, R.S., Araújo, C.V.M., Santos, L.V. de S., Moreira, V.R., Lebron, Y.A.R., Lange, L.C., 2021. The environmental risks of pharmaceuticals beyond traditional toxic effects: chemical differences that can repel or entrap aquatic organisms. Environ. Pollut. 268 https://doi.org/10.1016/j.envpol.2020.115902.
Jiang, Y., Pétrier, C., Waite, T.D., 2002. Effect of pH on the ultrasonic degradation of ionic aromatic compounds in aqueous solution. Ultrason. Sonochem. 9 (3), 163–168. https://doi.org/10.1016/S1350-4177(01)00114-6.
Kim, C., Thao, T.T., Kim, J.H., Hwang, I., 2020. Effects of the formation of reactive chlorine species on oxidation process using persulfate and nano zero-valent iron. Chemosphere 250, 126266. https://doi.org/10.1016/j.chemosphere.2020.126266.
Kishimoto, N., 2019. State of the art of UV/chlorine advanced oxidation processes: their mechanism, byproducts formation, process variation, and applications. J. Water Environ. Technol. 17 (5), 302–335. https://doi.org/10.2965/jwet.19-021.
Kuang, Y., Guo, X., Hu, J., Li, S., Zhang, R., Gao, Q., Yang, X., Chen, Q., Sun, W., 2020. Occurrence and risks of antibiotics in an urban river in northeastern Tibetan Plateau. Sci. Rep. 10 (1) https://doi.org/10.1038/s41598-020-77152-5.
Lai, X., Huang, N., Zhao, X., Li, Y., He, Y., Li, J., Deng, J., Ning, X. an, 2023. Oxidation of simulated wastewater by Fe2+-catalyzed system: the selective reactivity of chlorine radicals and the oxidation pathway of aromatic amines. Chemosphere 317 (November 2022), 137816. https://doi.org/10.1016/j.chemosphere.2023.137816.
Li, D., Feng, Z., Zhou, B., Chen, H., Yuan, R., 2022. Impact of water matrices on oxidation effects and mechanisms of pharmaceuticals by ultraviolet-based advanced oxidation technologies: a review. Sci. Total Environ. 844 (July), 157162 https://doi.org/10.1016/j.scitotenv.2022.157162.
Liu, P., Wu, Z., Abramova, A.V., Cravotto, G., 2021. Sonochemical processes for the degradation of antibiotics in aqueous solutions: a review. Ultrason. Sonochem. 74, 105566 https://doi.org/10.1016/j.ultsonch.2021.105566.
Lu, X., Zhou, X., Qiu, W., Wang, Z., Wang, Y., Zhang, H., Yu, J., Wang, D., Gu, J., Ma, J., 2022a. Kinetics and mechanism of the reaction of hydrogen peroxide with hypochlorous acid: implication on electrochemical water treatment. J. Hazard Mater. 438 (April), 129420 https://doi.org/10.1016/j.jhazmat.2022.129420.
Lu, Z., Ling, Y., Sun, W., Liu, C., Mao, T., Ao, X., Huang, T., 2022b. Antibiotics degradation by UV/chlor(am)ine advanced oxidation processes: a comprehensive review. Environ. Pollut. 308 (January), 119673 https://doi.org/10.1016/j.envpol.2022.119673.
Maghsodian, Z., Sanati, A.M., Mashifana, T., Sillanpää, M., Feng, S., Nhat, T., Ramavandi, B., 2022. Occurrence and distribution of antibiotics in the water, sediment, and biota of freshwater and marine environments: a review. Antibiotics 11 (11), 1–23. https://doi.org/10.3390/antibiotics11111461.
Medkova, D., Lakdawala, P., Hodkovicova, N., Blahova, J., Faldyna, M., Mares, J., Vaclavik, J., Doubkova, V., Hollerova, A., Svobodova, Z., 2022. Effects of different pharmaceutical residues on embryos of fish species native to Central Europe. Chemosphere 291 (P2), 132915. https://doi.org/10.1016/j.chemosphere.2021.132915.
Merouani, S., Hamdaoui, O., Saoudi, F., Chiha, M., Pétrier, C., 2010. Influence of bicarbonate and carbonate ions on sonochemical degradation of Rhodamine B in aqueous phase. J. Hazard Mater. 175 (1–3), 593–599. https://doi.org/10.1016/j.jhazmat.2009.10.046.
Mi, Y., Wang, N., Fang, X., Cao, J., Tao, M., Cao, Z., 2021. Interfacial polymerization nanofiltration membrane with visible light photocatalytic self-cleaning performance by incorporation of CQD/TiO2. Separ. Purif. Technol. 277 https://doi.org/10.1016/j.seppur.2021.119500.
Milne, L., Stewart, I., Bremner, D.H., 2013. Comparison of hydroxyl radical formation in aqueous solutions at different ultrasound frequencies and powers using the salicylic acid dosimeter. Ultrason. Sonochem. 20 (3), 984–989. https://doi.org/10.1016/j.ultsonch.2012.10.020.
Montoya-Rodríguez, D.M., Ávila-Torres, Y., Serna-Galvis, E.A., Torres-Palma, R.A., 2020a. Data on treatment of nafcillin and ampicillin antibiotics in water by sonochemistry. Data Brief 29, 105361. https://doi.org/10.1016/j.dib.2020.105361.
Montoya-Rodríguez, D.M., Serna-Galvis, E.A., Ferraro, F., Torres-Palma, R.A., 2020b. Degradation of the emerging concern pollutant ampicillin in aqueous media by sonochemical advanced oxidation processes - parameters effect, removal of antimicrobial activity and pollutant treatment in hydrolyzed urine. J. Environ. Manag. 261 (January), 110224 https://doi.org/10.1016/j.jenvman.2020.110224.
Moreno-Palacios, A.V., Palma-Goyes, R.E., Vazquez-Arenas, J., Torres-Palma, R.A., 2019. Bench-scale reactor for Cefadroxil oxidation and elimination of its antibiotic activity using electro-generated active chlorine. J. Environ. Chem. Eng. 7 (3), 103173 https://doi.org/10.1016/j.jece.2019.103173.
Papoutsakis, S., Afshari, Z., Malato, S., Pulgarin, C., 2015. Elimination of the iodinated contrast agent iohexol in water, wastewater and urine matrices by application of photo-Fenton and ultrasound advanced oxidation processes. J. Environ. Chem. Eng. 3 (3), 2002–2009. https://doi.org/10.1016/j.jece.2015.07.002.
Pétrier, C., Torres-Palma, R., Combet, E., Sarantakos, G., Baup, S., Pulgarin, C., 2010. Enhanced sonochemical degradation of bisphenol-A by bicarbonate ions. Ultrason. Sonochem. 17 (1), 111–115. https://doi.org/10.1016/j.ultsonch.2009.05.010.
Pignatello, J.J., Oliveros, E., MacKay, A., 2006a. Advanced oxidation processes for organic contaminant destruction based on the fenton reaction and related chemistry. Crit. Rev. Environ. Sci. Technol. 36 (1), 1–84. https://doi.org/10.1080/10643380500326564.
Pignatello, J.J., Oliveros, E., MacKay, A., 2006b. Advanced oxidation processes for organic contaminant destruction based on the fenton reaction and related chemistry. Crit. Rev. Environ. Sci. Technol. 36 (1), 1–84. https://doi.org/10.1080/10643380500326564.
Pirsaheb, M., Moradi, N., 2020. Sonochemical degradation of pesticides in aqueous solution: Investigation on the influence of operating parameters and degradation pathway-a systematic review. RSC Adv. 10 (13), 7396–7423. https://doi.org/10.1039/c9ra11025a.
Podio, N.S., Bertrand, L., Wunderlin, D.A., Santiago, A.N., 2020. Assessment of phytotoxic effects, uptake and translocation of diclofenac in chicory (Cichorium intybus). Chemosphere 241. https://doi.org/10.1016/j.chemosphere.2019.125057.
Quimbaya-Ñañez, C., Serna-Galvis, E.A., Silva-Agredo, J., Huerta, L., Torres-Palma, R.A., Ávila-Torres, Y., 2024. Mn-based material derived from industrial sawdust for the elimination of ciprofloxacin: loss of antibiotic activity and toxicity via carbocatalysis assisted by ultrasound. J. Environ. Chem. Eng. 12 (2), 112015 https://doi.org/10.1016/j.jece.2024.112015.
Rahmani, A.R., Mousavi-Tashar, A., Masoumi, Z., Azarian, G., 2019. Integrated advanced oxidation process, sono-Fenton treatment, for mineralization and volume reduction of activated sludge. Ecotoxicol. Environ. Saf. 168 (October 2018), 120–126. https://doi.org/10.1016/j.ecoenv.2018.10.069.
Rayaroth, M.P., Aravindakumar, C.T., Shah, N.S., Boczkaj, G., 2022. Advanced oxidation processes (AOPs) based wastewater treatment - unexpected nitration side reactions - a serious environmental issue: a review. Chem. Eng. J. 430 https://doi.org/10.1016/j.cej.2021.133002. Elsevier B.V.
Ribeiro, A.R., Sures, B., Schmidt, T.C., 2018. Cephalosporin antibiotics in the aquatic environment: a critical review of occurrence, fate, ecotoxicity and removal technologies. Environ. Pollut. 241, 1153–1166. https://doi.org/10.1016/j.envpol.2018.06.040.
Sathishkumar, P., Mangalaraja, R.V., Anandan, S., 2016. Review on the recent improvements in sonochemical and combined sonochemical oxidation processes - a powerful tool for destruction of environmental contaminants. Renew. Sustain. Energy Rev. 55 (March), 426–454. https://doi.org/10.1016/j.rser.2015.10.139.
Serna-Galvis, E.A., Montoya-Rodríguez, D., Isaza-Pineda, L., Ibáñez, M., Hernández, F., Moncayo-Lasso, A., Torres-Palma, R.A., 2019. Sonochemical degradation of antibiotics from representative classes-Considerations on structural effects, initial transformation products, antimicrobial activity and matrix. Ultrason. Sonochem. 50, 157–165. https://doi.org/10.1016/j.ultsonch.2018.09.012.
Serna-Galvis, E.A., Porras, J., Torres-Palma, R.A., 2022. A critical review on the sonochemical degradation of organic pollutants in urine, seawater, and mineral water. Ultrason. Sonochem. 82 (August 2021), 105861 https://doi.org/10.1016/j.ultsonch.2021.105861.
Serna-Galvis, E.A., Silva-Agredo, J., Giraldo-Aguirre, A.L., Torres-Palma, R.A., 2015. Sonochemical degradation of the pharmaceutical fluoxetine: effect of parameters,

organic and inorganic additives and combination with a biological system. Sci. Total Environ. 524–525, 354–360. https://doi.org/10.1016/j.scitotenv.2015.04.053.
Serna-Galvis, E.A., Silva-Agredo, J., Giraldo, A.L., Flórez, O.A., Torres-Palma, R.A., 2016. Comparison of route, mechanism and extent of treatment for the degradation of a β-lactam antibiotic by TiO2 photocatalysis, sonochemistry, electrochemistry and the photo-Fenton system. Chem. Eng. J. 284, 953–962. https://doi.org/10.1016/j.cej.2015.08.154.
Supeno, Kruus, P., 2000. Sonochemical formation of nitrate and nitrite in water. Ultrason. Sonochem. 7 (3), 109–113. https://doi.org/10.1016/S1350-4177(99)00043-7.
Uzzaman, M., Shawon, J., Siddique, Z.A., 2019. Molecular docking, dynamics simulation and ADMET prediction of Acetaminophen and its modified derivatives based on quantum calculations. SN Appl. Sci. 1 (11) https://doi.org/10.1007/s42452-019-1442-z.
Vassilakis, C., Pantidou, A., Psillakis, E., Kalogerakis, N., Mantzavinos, D., 2004. Sonolysis of natural phenolic compounds in aqueous solutions: degradation pathways and biodegradability. Water Res. 38 (13), 3110–3118. https://doi.org/10.1016/j.watres.2004.04.014.
Villaroel, E., Silva-Agredo, J., Petrier, C., Taborda, G., Torres-Palma, R.A., 2014. Ultrasonic degradation of acetaminophen in water: effect of sonochemical parameters and water matrix. Ultrason. Sonochem. 21 (5), 1763–1769. https://doi.org/10.1016/j.ultsonch.2014.04.002.
Villegas-Guzman, P., Silva-Agredo, J., Giraldo-Aguirre, A.L., Flórez-Acosta, O., Petrier, C., Torres-Palma, R.A., 2015. Enhancement and inhibition effects of water matrices during the sonochemical degradation of the antibiotic dicloxacillin. Ultrason. Sonochem. 22, 211–219. https://doi.org/10.1016/j.ultsonch.2014.07.006.
Wang, L., Zhu, L., Luo, W., Wu, Y., Tang, H., 2007. Drastically enhanced ultrasonic decolorization of methyl orange by adding CCl4. Ultrason. Sonochem. 14 (2), 253–258. https://doi.org/10.1016/j.ultsonch.2006.05.004.
Wei, H., Shi, J., Yang, X., Wang, J., Li, K., He, Q., 2018. CCl 4 -enhanced ultrasonic irradiation for ciprofloxacin degradation and antibiotic activity. Water Environ. Res. 90 (7), 579–588. https://doi.org/10.2175/106143017x15131012153077.
Won, J.S., Kaewsuk, J., Jo, J.H., Lim, D.H., Seo, G.T., 2015. A density functional theory study on the ozone oxidation of sulfonamide antibiotics. J. Adv. Oxid. Technol. 18 (1), 31–38. https://doi.org/10.1515/jaots-2015-0104.
Yang, L., Sostaric, J.Z., Rathman, J.F., Weavers, L.K., 2008. Effect of ultrasound frequency on pulsed sonolytic degradation of octylbenzene sulfonic acid. J. Phys. Chem. B 112 (3), 852–858. https://doi.org/10.1021/jp077482m.
Zare, M., Alfonso-muniozguren, P., Bussemaker, M.J., Sears, P., Serna-galvis, A., Torres-palma, R.A., Lee, J., 2023. Ultrasonics Sonochemistry A fundamental study on the degradation of paracetamol under single- and dual-frequency ultrasound. Ultrason. Sonochem. 94 (December 2022), 106320 https://doi.org/10.1016/j.ultsonch.2023.106320.